



Kinetics of the $\beta \rightarrow \delta$ solid–solid phase transition of HMX, octahydro-1,3,5,7-tetranitro-1,3,5,7-tetrazocine

R.K. Weese^{a,*}, J.L. Maienschein^a, C.T. Perrino^b

^a Lawrence Livermore National Laboratory, Livermore, CA 94550, USA

^b Chemistry Department, California State University at Hayward, Hayward, CA 94542, USA

Received 22 November 2001; received in revised form 2 August 2002; accepted 17 August 2002

Abstract

We apply differential scanning calorimetry (DSC) to measure the kinetics of the $\beta \rightarrow \delta$ solid–solid phase transition of octahydro-1,3,5,7-tetranitro-1,3,5,7-tetrazocine, HMX. Integration of the DSC signal gives a direct measurement of degree of conversion. Data is analyzed by first-order kinetics, the Ozawa method, and isoconversional analysis. The range of activation energies found in this work, centering around 500 kJ/mol, is much higher than previously reported values by Brill and co-workers [AIAA J. (1982)], 204 kJ/mol [1], and Henson et al. and Henson and co-workers [B. Henson, L. Smilowitz, B. Asay, P. Dickson, Thermodynamics of the beta to delta phase transition in PBX-9501, in: Proceedings of American Physical Society Topical Group on Shock Compression of Condensed Matter, American Institute of Physics, Atlanta, GA, 2001; L. Smilowitz, B. Henson, J. Robinson, P. Dickson, B. Asay, Kinetics of the beta to delta phase transition in PBX-9501, in: Proceedings of American Physical Society Topical Group on Shock Compression of Condensed Matter, American Institute of Physics, Atlanta, GA, 2001; P.M. Dickson, B.W. Asay, B.F. Henson, C.S. Fugard, J. Wong, Measurement of phase change and thermal decomposition kinetics during cookoff of PBX-9501, in: Proceedings of American Physical Society Topical Group on Shock Compression of Condensed Matter, American Institute of Physics, Snowbird, UT, 1999], 200 kJ/mol [4]. We discuss possible reasons for the higher activation energies measured here but do not identify the cause.

© 2003 Published by Elsevier Science B.V.

Keywords: Solid–solid phase; Transition; HMX

1. Introduction

The chemical compound octahydro-1,3,5,7-tetranitro-1,3,5,7-tetrazocine, HMX, is an high-performance nitramine energetic material. HMX exists in four solid phase polymorphs, labeled α , β , γ , δ -HMX [5,6], each of which can reportedly be prepared by a specific cooling rate of a reaction solution [7]. The β phase of HMX has the highest density and is stable

at room temperature; it is the form in which HMX is normally produced and used. However, when heated to temperatures above 435 K, the β phase converts to δ phase HMX [5,8–11].

This conversion of the β phase (monoclinic lattice structure) to the δ phase (hexagonal lattice structure) involves a major disruption of the cohesive forces in the HMX crystal lattice and a ring conformation change from β (chair) to δ (chair–chair) [12,13]. The electrostatic forces created within the HMX lattice produce a potential energy barrier to overcome in the transformation from the $\beta \rightarrow \delta$ phase [9]. The energy to bring about the change from chair to chair–chair

* Corresponding author. Tel.: +1-925-424-3165;

fax: +1-925-424-3281.

E-mail address: weese2@llnl.gov (R.K. Weese).

conformation has been reported by Brill [12] as ring torsion and is essentially a normal mode of the molecule that requires about 4 kJ mol^{-1} .

The β and δ phases of HMX have quite different behaviors. For example, the volume expansion associated with the $\beta \rightarrow \delta$ phase transition (the density is 1.90 for β and 1.78 g/cm^3 for δ) produces profound perturbations to the mechanical and combustion characteristics of HMX [8,9,14,15]. The higher density material shows a higher rate of detonation and maintains greater stability towards shock. In sensitivity to mechanical impact as assessed by a standard drop-weight impact test such as described by Dobratz [16], δ phase HMX is significantly more sensitive than β phase HMX [5,14]. It is therefore desirable to know the kinetic information associated with this $\beta \rightarrow \delta$ solid phase transition. Data have been reported by Brill [9,17,18] and by Henson [2,3] using FTIR and second harmonic generation, respectively, to monitor the transition extent. Their energies were observed to be 204 and 200 kJ/mol. Here we investigate the kinetics of the $\beta \rightarrow \delta$ solid phase transition in HMX using differential scanning calorimetry (DSC) and determine kinetic rate parameters and an effective activation energy. Our activation energy of $\sim 500 \text{ kJ/mol}$ is much higher than previous values, and a possible reason is discussed.

2. Experimental method and calibration

The instrument used for making DSC measurements in this work is a TA Instruments Model 2920 [19].

The DSC was calibrated at each ramp rate for temperature and heat flow and to reduce baseline drift. Indium, lead, tin, and zinc were used for temperature calibration, and the indium heat of fusion was used for heat flow calibration. The instrumental error was $\leq 1.4^\circ\text{C}$ in temperature and $\leq 2.0\%$ in heat flow, typical for this type of measurement.

We recorded DSC data at heating rates of 1, 2, 5, and 10°C/min , with sample masses of about 1 mg. The thermal ramp was extended to a temperature sufficient to bring the phase conversion to completion, but was stopped below the temperature where the HMX would exothermically react. We made four runs at each heating rate. The lids of the DSC sample pans were perforated, to maintain the sample at atmospheric pressure. All data reported with exotherm up.

The HMX used in these experiments was recrystallized from standard-grade HMX, and was 99% pure as measured by HPLC. The average particle size was $160 \mu\text{m}$ with the central 80% being between 30 and $300 \mu\text{m}$, and the sample masses ranged from 0.81 to 1.29 mg, with most around 1.1 mg.

3. Results and discussion

The $\beta \rightarrow \delta$ transition in HMX is endothermic, and is readily measured by DSC. Typical data are shown in Figs. 1–4 for the different heating rates.

The data in Figs. 1–4 have significant fine structure superimposed on the main thermal event, particularly at the lower heating rates. We conjecture that this is due to uneven contact of the powdered sample with the sample pan, with resulting variations in thermal contact efficiency and therefore heat flow. This would be expected from the change in crystal morphology and density during the phase transition, with different particles undergoing transition at slightly different times and thereby adding a random structure

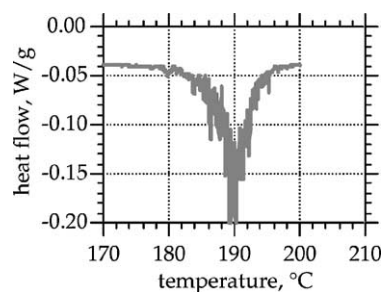


Fig. 1. DSC data for 1°C/min , heating rate, #99-896.01.

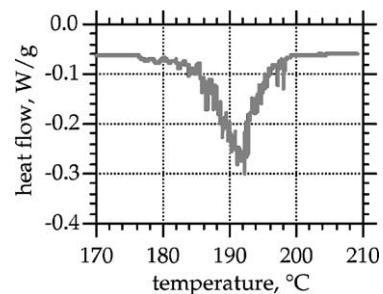


Fig. 2. DSC data for 2°C/min , heating rate, #99-890.01.

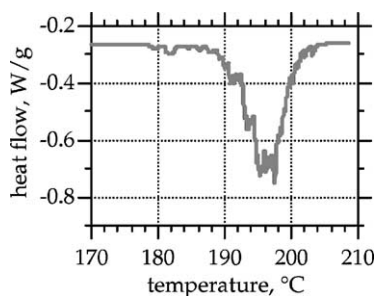


Fig. 3. DSC data for 5 °C/min, heating rate, #99-878.01.

to the overall thermal signature. The presence of this fine structure does not preclude kinetic analysis of the data, but could introduce noise in the isoconversional analysis.

The DSC data can be converted to fractional conversion by:

$$\alpha_t = \frac{\Delta H_t}{\Delta H_{\text{tot}}} \quad (1)$$

where α_t is the reaction extent at time t ; H_t the total heat of reaction at time t , calculated by integrating the DSC signal up to time t ; H_{tot} the total heat of reaction, calculated by integrating the DSC signal over the entire phase transition.

The reaction rate can then be written as:

$$\frac{d\alpha}{dt} = \left(\frac{d(\Delta H_t)}{dt} \right) \times \left(\frac{1}{\Delta H_{\text{tot}}} \right) = \frac{dQ}{dt} \times \left(\frac{1}{\Delta H_{\text{tot}}} \right) \quad (2)$$

where dQ/dt is the heat flow given by the DSC signal.

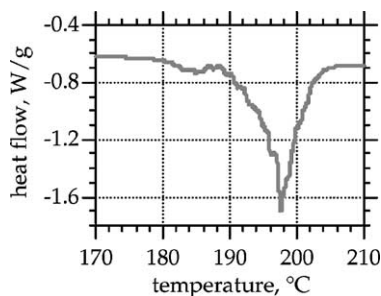


Fig. 4. DSC data for 10 °C/min, heating rate, #99-872.01.

3.1. Calculation of Arrhenius parameters—first-order assumption

The reaction rate may also be written, for a simple n th-order reaction with Arrhenius kinetics, as:

$$\frac{d\alpha}{dt} = k(1 - \alpha)^n = A e^{-E_A/RT} (1 - \alpha)^n \quad (3)$$

where k is the reaction rate constant (s^{-1}); A the Arrhenius pre-exponential (s^{-1}); E_A the activation energy (kJ/mol); n the reaction-order.

Combining Eqs. (2) and (3), we can calculate the instantaneous rate constant as a function of temperature for a given DSC run by:

$$k = \frac{dQ}{dt} \times \left(\frac{1}{\Delta H_{\text{tot}}} \right) \times (1 - \alpha)^{-n} \quad (4)$$

We analyzed each DSC run in the following way. First, we integrated the total phase transition signal to determine the total heat of reaction. Then, the reaction extent as a function of time was calculated using Eq. (1). Finally, the reaction rate constant was calculated as a function of time for reaction extents using Eq. (4), assuming first-order kinetics. A representative plot of the rate constant as a function of time for one run is shown in Fig. 5. For each run, we calculated an average rate constant near mid conversion. These mean values are shown in Table 1, and plotted in Fig. 5. The resulting activation energy is 433 ± 13 kJ/mol, and the pre-exponential term is $2 \times 10^{48} s^{-1}$.

From Fig. 5, we see that the rate constant during a DSC run is not linear. This could be due to a couple of effects. First, the temperature is not constant during the course of the run, so the rate constant would be expected to increase exponentially. The data in Fig. 5

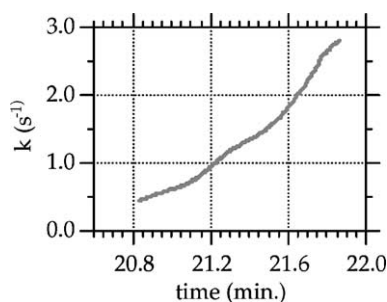


Fig. 5. Rate constant calculated from Eq. (4) for run 878.01 at 5 °C/min.

Table 1

Mean rate constants and temperatures for each thermal ramp rate

Ramp rate (°C/min)	k (s ⁻¹)	T (K)
1	0.208	463.1
2	0.363	465.4
5	0.843	468.7
10	1.41	471.3

The values represent averages of four runs at each ramp rate.

span about 1 min or 5 K. Applying the activation energy of 433 kJ/mol to the minimum and maximum temperatures represented in Fig. 5, 466.2–471.2 K, we calculate that the rate constant should vary by a factor of 3.3. This is a significant portion of the overall variation of a factor of 6.5, but does not account for all of the variation. A changing rate constant indicates that the reaction is not a simple first-order reaction. Nucleation reactions would have a greater increase over the interval, and they may be appropriate for this transformation. Our method of using the rate constant at the peak of the endotherm is therefore an approximation, and our kinetic constants calculated in this manner must therefore be considered estimates.

3.2. Calculation of Arrhenius parameters—Ozawa method

An alternate method of calculating kinetic parameters is the method of Ozawa, wherein the thermal ramp rate as a function of the peak temperature is used for conventional Arrhenius analysis [20,21]. This gives directly an estimate of the activation energy. The ramp rate and peak temperature data are shown in Arrhenius form in Fig. 6. The activation energy, 510 kJ/mol,

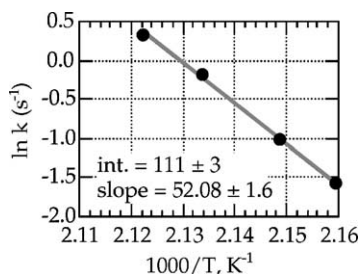


Fig. 6. Arrhenius plot of kinetic data from Table 1. Activation energy is 433 kJ/mol, and the pre-exponential term is $2 \times 10^{48} \text{ s}^{-1}$.

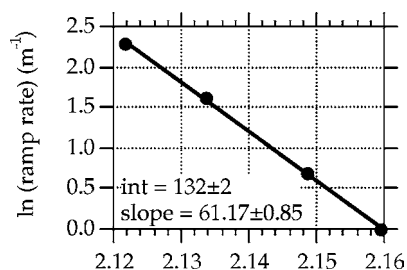


Fig. 7. Ramp rate vs. $1/T$ (K) \times 1000.

is significantly higher than that calculated above from the actual reaction rate data.

3.3. Calculation of Arrhenius parameters—isoconversional analysis

The above methods for calculating activation energy assume an unchanging reaction mechanism with first-order reaction. Similar analyses can be made with different reaction-orders that lead to different kinetic parameters; it is often difficult if not impossible to determine which is the appropriate reaction-order from this type of analysis [21]. Furthermore, if the reaction mechanism changes during the course of the reaction, the above methods can only give a global average that may not truly represent any of the actual mechanistic steps.

Fig. 7 is the natural logarithm of the ramp rate and inverse peak temperature data, with a linear fit for calculating activation energy.

Isoconversional analysis is an alternate method of kinetic analysis that avoids these problems [22–25]. In isoconversional analysis, data from several different ramp rates are required. For each ramp rate, the reaction rate and temperature is determined for different extents of reaction; then the Arrhenius parameters are calculated from the set of temperature-rate data at each reaction extent. Changes in the activation energy with reaction extent indicate changes in reaction mechanisms. The pre-exponential parameter lumps together all reaction-order effects, and so its behavior also may give insight into the actual mechanisms. There is no assumption of reaction-order inherent in isoconversional analysis [26], so the activation energies should be representative of the actual reactions taking place.

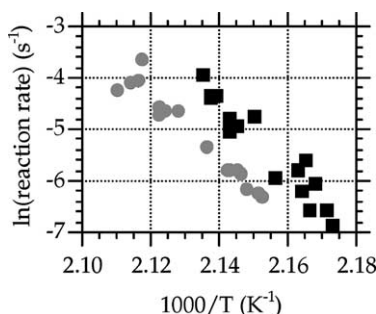


Fig. 8. Reaction rates as a function of temperature at reaction extents of 0.2 (square) and 0.8 (circle).

Steps in the isoconversional analysis were: (1) calculate the reaction extent from integration of the DSC data, using evenly-spaced temperature data over the same temperature range for each run at given ramp rate; (2) interpolate the temperature/reaction extent data sets to give temperature/reaction extent data at evenly spaced reaction extent values ranging from 0.01 to 0.99; (3) calculate the reaction rate for each reaction extent value from the temperature/reaction extent/ramp rate data; (4) for each reaction extent, use rate/temperature data from the four ramp rates to calculate Arrhenius parameters as a function of reaction extent. Typical results at reaction extents of 0.2 and 0.8 are shown in Fig. 8, and the resulting Arrhenius activation energy and pre-exponential values are shown in Figs. 9–12 for reaction extents from 0.05 to 0.95. Average activation energy of 488 kJ mol^{-1} was observed, a standard deviation of 23 kJ mol^{-1} was determined for this data set, approximately 5% difference. Typically errors associated with measurements of this type are two parts in 100. Systematic errors of this type may

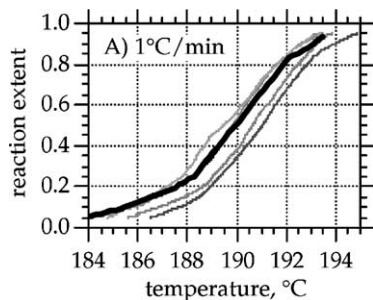


Fig. 9. Reaction extent vs. temperature at 1°C/min .

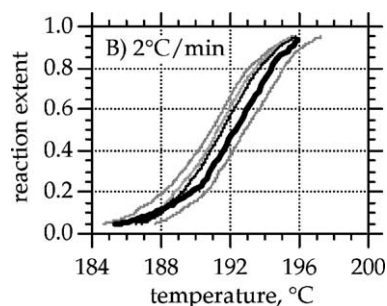


Fig. 10. Reaction extent vs. temperature at 2°C/min .

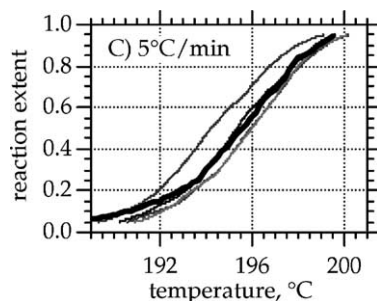


Fig. 11. Reaction extent vs. temperature at 5°C/min .

have contributed to the noise in the data that caused the errors associated with the activation energy.

As a check of the validity of the values, we used these parameters to calculate the reaction extent as a function of temperature for the four experimental ramp rates, and then compared the calculated values with the experimental data. This is shown in Fig. 8. The agreement is excellent, with the calculated reaction extent fitting well within the envelope of experimental results for each ramp rate. We note that to achieve the

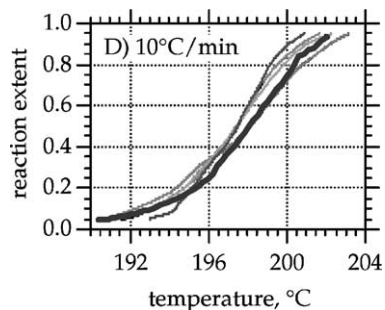


Fig. 12. Reaction extent vs. temperature at 10°C/min .

degree of agreement some of the Arrhenius parameters derived from Fig. 9 were adjusted to the nearest 0.5 kJ/mol or s⁻¹. The adjustments were small in all cases, and the adjusted parameters are still consistent with the data shown in Fig. 9.

Figs. 9–12 show the reaction extents of the phase transition. For Figs. 9–12 all measured values—solid lines. Calculated from Arrhenius parameters—thick dotted line. Each plot is for the thermal ramp rate shown on the plot.

From the data available we cannot determine a mechanistic scheme.

The activation energies for the different steps in the reaction are quite high—465–538 kJ/mol. These values are consistent with those from our simpler analyses presented earlier—433 kJ/mol for the first-order assumption and 510 kJ/mol using the Ozawa method, showing a general agreement among the three methods of analysis.

3.4. Comparison with literature

With pure HMX and using FTIR spectroscopy to monitor the $\beta \rightarrow \delta$ phase transition, Brill et al. observed first-order kinetics and determined activation energy of 204 kJ/mol [23]. Henson et al. studies HMX mixed with estane and nitroplasticizers (PBX-9501), using second harmonic generation of reflected light to measure the reaction extent [2,3,25]. He built a model for the transition based on a nucleation and growth mechanism with a first-order nucleation step and a second-order growth step; activation energies were on the order of 200 kJ/mol for each step.

Our results show that the reaction is not a simple first-order reaction. First, the range of activation energies that we find, around 500 kJ/mol, are significantly higher than those found by Brill and by Henson and are too high to be physically reasonable. Second, the reaction profile is even narrower than predicted by the 500 kJ/mol energy. The reasons for this are not fully understood. The most likely explanation is that the results are influenced by the thermodynamics of the phase change. In the limit of a pure thermodynamic control, the peak in the reaction profile would be independent of heating rate as long as heat transfer contributions were properly accounted for. That would lead to infinite activation energy by both the Ozawa and isoconversional methods. In

a mixed thermodynamic-kinetic regime, the apparent activation energy would be higher than the true value.

4. Conclusions

We have monitored the reaction progress of the HMX $\beta \rightarrow \delta$ phase transition using differential scanning calorimetry and pure HMX, and analyzed the results using three methods—assuming first-order kinetics, the Ozawa method, and isoconversional analysis. Although the three methods used for determination of the activation energy were in agreement, agreement does not guarantee validity—there is still the question of whether this is truly a chemical kinetic measurement.

The activation energies with different analytical methods are all around 500 kJ/mol, significantly higher than reported in the literature. As discussed above, this may be the result of thermodynamic influences on the reaction rates.

Reported E_A energies for solid–solid transition are typically on the order of 125–150 kJ/mol and the actual reaction mechanisms of some solid-state reactions may be too complex to be described by the kinetic triplet [26].

Acknowledgements

This work was performed under the auspices of the US Department of Energy by the University of California Lawrence Livermore National Laboratory under contract No. W-7405-Eng-48.

References

- [1] R.J. Karpowicz, L.S. Gelfand, T.B. Brill, Application of solid-phase transition kinetics to the properties of HMX, AIAA J., 1982.
- [2] B. Henson, L. Smilowitz, B. Asay, P. Dickson, Thermodynamics of the beta to delta phase transition in PBX-9501, in: Proceedings of American Physical Society Topical Group on Shock Compression of Condensed Matter, American Institute of Physics, Atlanta, GA, 2001.
- [3] L. Smilowitz, B. Henson, J. Robinson, P. Dickson, B. Asay, Kinetics of the beta to delta phase transition in PBX-9501, in: Proceedings of American Physical Society Topical Group on

- Shock Compression of Condensed Matter, American Institute of Physics, Atlanta, GA, 2001.
- [4] P.M. Dickson, B.W. Asay, B.F. Henson, C.S. Fugard, J. Wong, Measurement of phase change and thermal decomposition kinetics during cookoff of PBX-9501, in: Proceedings of American Physical Society Topical Group on Shock Compression of Condensed Matter, American Institute of Physics, Snowbird, UT, 1999.
- [5] H.H. Cady, Studies on the Polymorphs of HMX, LAMS-2652, Los Alamos Scientific Laboratory, 1961.
- [6] R.E. Cobblestick, R.W.H. Small, The crystal structure of the d-form of 1,3,5,6-tetranitro-1,3,5,7-tetraazacyclooctane (d-HMX), *Acta Cryst.* B30 (1974) 1918.
- [7] W.C. McCrone, Crystallographic data: cyclotetramethylene tetranitramine (HMX), *Anal. Chem.* 22 (1950) 1225.
- [8] M. Herrmann, W. Engel, N. Eisenreich, Phase transitions of HMX and their significance for the sensitivity of explosives, in: Proceedings of the Technical Meeting of Specialists MWDDEA AF-71-F/G-7304—Physics of Explosives, 1990, p. 12.
- [9] R.J. Karpowicz, T.B. Brill, The baed transformation of HMX: its thermal analysis and relationship to propellants, *AIAA J.* 20 (1982) 1586.
- [10] A.S. Teetsov, W.C. McCrone, The microscopical study of polymorph stability diagrams, *Microsc. Cryst. Front.* 15 (1965) 13.
- [11] M. Herrmann, W. Engel, N. Eisenreich, Thermal analysis of the phases of HMX using X-ray diffraction, *Zeitschrift für Kristallographie* 204 (1993) 121.
- [12] T.B. Brill, R.J. Karpowicz, Solid phase transition kinetics: the role of intermolecular forces in the condensed phase decomposition of octahydro-1,3,5,7-tetranitro-1,3,5,7-tetrazocine, *J. Phys. Chem.* 86 (1982) 4260.
- [13] T.B. Brill, C.O. Reese, Analysis of intermolecular interactions relating in the thermophysical behavior of alpha, beta, and delta octahydro-1,3,5,7-tetranitro-1,3,5,7-tetrazocine, *J. Phys. Chem.* 84 (1980).
- [14] M. Herrmann, W. Engel, N. Eisenreich, Thermal expansion, transitions, sensitivities and burning rates of HMX, *Propel. Explos. Pyrotech.* 17 (1992) 190.
- [15] J.L. Maienschein, J.B. Chandler, Burn rates of pristine and degraded explosives at elevated pressures and temperatures, in: Proceedings of 11th International Detonation Symposium, Office of Naval Research, Snowmass, CO, 1998.
- [16] B.M. Dobratz, P.C. Crawford, LLNL Explosives Handbook: Properties of Chemical Explosives and Explosive Stimulants, UCRL-52997 Change 2, Lawrence Livermore National Laboratory, 1985.
- [17] F. Goetz, T.B. Brill, Laser Raman spectra of a-, b-, g, and d-octahydro-1,3,5,7-tetranitro-1,3,5,7-tetrazocine and their temperature dependence, *J. Phys. Chem.* 83 (1979) 340.
- [18] A.G. Landers, T.B. Brill, Pressure–temperature dependence of the baed polymorph interconversion in octahydro-1,3,5,7-tetranitro-1,3,5,7-tetrazocine, *J. Phys. Chem.* 84 (1980) 3573.
- [19] TA Instruments, Instrument Manual.
- [20] T. Ozawa, Kinetic analysis of derivative curves in thermal analysis, *J. Thermal Anal.* 2 (1970) 301.
- [21] S. Vyazovkin, C.A. Wight, Isothermal and non-isothermal kinetics of thermally stimulated reactions of solids, *Int. Rev. Phys. Chem.* 17 (1998) 407.
- [22] S. Vyazovkin, C.A. Wight, Estimating realistic confidence intervals for the activation energy determined from thermo-analytical measurements, *Anal. Chem.* 72 (2000) 3171.
- [23] J.H. Flynn, The isoconversional method for determination of energy of activation at constant heating rates. Corrections for the Doyle approximation, *J. Thermal Anal.* 27 (1983) 95.
- [24] H.L. Friedman, Kinetics of thermal degradation of char-forming plastics from thermogravimetry. Application to a phenolic plastic, *J. Polymer Sci. C* 6 (1963) 183.
- [25] V.A. Bershtein, V.M. Ergorov, Differential Scanning Calorimetry of Polymers, Ellis Horwood Ltd., Chichester, 1994.
- [26] M.E. Brown, M. Maciejewski, S. Vyazovkin, R. Nomem, Computational aspects of kinetic analysis Part A: the ICTAC kinetics project-data, *Thermochim. Acta* 355 (2000) 125–143.